

## Preparation of nanocrystalline GZO/CdS bilayer films using magnetron sputtering and GZO/CdS/p-Si heterojunction photovoltaic device

HE Bo<sup>1,2\*</sup>, XU Jing<sup>3</sup>, NING Huan-Po<sup>1</sup>, XING Huai-Zhong<sup>1</sup>, WANG Chun-Rui<sup>1</sup>,  
ZHANG Xiao-Dong<sup>1</sup>, MO Guan-Kong<sup>4</sup>, SHEN Xiao-Ming<sup>4</sup>

(1. Department of Applied Physics, Donghua University, Shanghai, 201620, China;

2. Institute for Energy Technology, Instituttveien 18, 2007 Kjeller, Norway;

3. Instrumental Analysis and Research Center, Shanghai University, Shanghai 200444, China;

4. School of Resources, Environment and Materials, Guangxi University, Nanning 530004, China)

**Abstract:** In this work, Ga doped ZnO (GZO)/CdS bilayer films were prepared on p-Si substrate by magnetron sputtering to form GZO/CdS/p-Si heterojunction device. The structural, optical and electrical properties of the nanocrystalline GZO/CdS bilayer films were studied by XRD, SEM, XPS, UV-VIS spectrophotometer and Hall effect measurement. The J-V curve of GZO/CdS/p-Si heterojunction device shows good rectifying behavior. And the value of  $I_F/I_R$  ( $I_F$  and  $I_R$  stand for forward and reverse current, respectively) at  $\pm 3$  V is found to be as high as 21. The results indicate that the nanocrystalline GZO/CdS/p-Si heterojunction possesses good diode characteristic. High photocurrent density is obtained under a reverse bias. The nanocrystalline GZO/CdS/p-Si heterojunction device exhibits clear photovoltaic effect. Because the lattice constant of CdS is between GZO and Si, it can be used for a buffer layer between GZO and Si, to effectively reduce the interface states between GZO and p-Si. Therefore, we observed the clear photovoltaic effect of GZO/CdS/p-Si heterojunction.

**Key words:** nanocrystalline GZO/CdS bilayer films, magnetron sputtering, heterojunction, current-voltage ( $I$ - $V$ ) characteristics

**PACS:** 78.67.Bf

## 磁控溅射制备纳米晶 GZO/CdS 双层膜及 GZO/CdS/p-Si 异质结光伏器件的研究

何波<sup>1,2\*</sup>, 徐静<sup>3</sup>, 宁欢颇<sup>1</sup>, 邢怀中<sup>1</sup>, 王春瑞<sup>1</sup>, 张晓东<sup>1</sup>, 莫观孔<sup>4</sup>, 沈晓明<sup>4</sup>

(1. 东华大学 应用物理系, 上海 201620;

2. 挪威能源技术研究所, Instituttveien 18, 2007 Kjeller;

3. 上海大学 分析测试中心, 上海 200444;

4. 广西大学 资源环境与材料学院, 广西 南宁 530004)

**摘要:** 采用磁控溅射制备 Ga 掺杂 ZnO (GZO)/CdS 双层膜在 p 型晶硅衬底上以形成 GZO/CdS/p-Si 异质结器件。纳米晶 GZO/CdS 双层膜的微结构、光学及电学特性, 通过 XRD、SEM、XPS、紫外-可见光分光光度计和霍尔效应测试系统表征。GZO/CdS/p-Si 异质结 J-V 曲线显示良好的整流特性。在  $\pm 3$  V 时, 整流比  $I_F/I_R$  ( $I_F$  和  $I_R$  分别表示正向和反向电流) 已达到 21。结果表明纳米晶 GZO/CdS/p-Si 异质结具有好的二极管特性, 在反向偏压下获得高光电流密度。纳米晶 GZO/CdS/p-Si 异质结显示明显的光伏特性。由于 CdS 晶格常数在 GZO 和晶 Si 之间, 它能作为一个介于 GZO 和晶 Si 之间的缓冲层, 能有效地减少 GZO 和 p-Si 之间的界面态。因此, 我们获得了 GZO/CdS/p-Si 异质结明显光伏特性。

**Received date:** 2018-06-30, **revised date:** 2018-12-25

**收稿日期:** 2018-06-30, **修回日期:** 2018-12-25

**Foundation items:** Supported by Fund PLA General Armament Department "The 15th Five-year" weapons and Equipments Pre-research Field Foundation "Basic application technology of graphene materials in batteries" (6140721040412)

**Biography:** HE Bo (1981-), male, China, a teacher in Department of Applied Physics, Donghua University. post-doctor of materials science and engineering in Donghua University. Research is mainly about semiconductor photoelectric materials and devices. E-mail: laserhebo@163.com

\* **Corresponding author:** E-mail: laserhebo@163.com

关键词: 纳米晶 GZO/CdS 双层膜; 磁控溅射; 异质结; 电流-电压 (*I-V*) 特性

中图分类号: 04 文献标识码: A

## Introduction

In recent years, transparent conducting oxide (TCO)/Si heterojunction solar cells have received increasing attention<sup>[1-3]</sup>, because the device structure is simple, cheap and not using pn junction.

Zinc oxide (ZnO) is a very important II-VI compound semiconductor material with direct wide bandgap of 3.3 eV. It can be used for various photoelectronic applications such as flat panel displays, liquid crystal displays, organic light emitting diodes, thin film transistors and thin film solar cells. It has many merits such as abundance in natural resource, low cost, non-toxicity and high stability. ZnO naturally shows n-type conduction and the electrical behaviour of ZnO thin films could be significantly improved by replacing Zn atoms with higher valence elements, such as B, In, Al and Ga<sup>[4-9]</sup>. Ga doped ZnO (GZO) film has more advantages than Al doped ZnO (AZO) film. Because the radius of Ga<sup>3+</sup> ion and Zn<sup>2+</sup> ion are similar, it leads to only a small lattice deformation. Compared to aluminum, gallium is less reactive and oxidative. GZO films are more stable than AZO films. However, GZO has been relatively less researched than AZO.

Cadmium Sulfide (CdS) is an important II-VI compound semiconductor optoelectric material. It has an ideal energy band gap of 2.4 eV. Many techniques have been used to grow CdS films: magnetron sputtering<sup>[10]</sup>, PLD<sup>[11]</sup>, ultrasonic spray method<sup>[12]</sup>, sol-gel<sup>[13]</sup> and so on. Among these techniques, magnetron sputtering is simple, convenient and fast for large area deposition of polycrystalline CdS film.

However, the lattice mismatch between ZnO and Si is as high as 40%. According to some research, the efficiency of ZnO/p-Si heterojunction is low. For example, L Li *et al.* reported that under AM1.5G (100 mW/cm<sup>2</sup>) sunlight illumination, the open-circuit voltage ( $V_{oc}$ ) of the n-ZnO/p-Si heterojunction made by molecular beam epitaxy (MBE) is 131 mV<sup>[14]</sup>. This shows that the photovoltaic characteristics of n-ZnO/p-Si heterojunctions are facing great challenges. In order to improve the photovoltaic characteristics of n-ZnO/p-Si heterojunction, CdS can be used as a buffer layer, since the lattice constant of CdS is between ZnO and Si. On the other hand, Ga doped ZnO (GZO) film with low resistivity and high transmittance in the visible region can be used as a top transparent collecting electrode.

In this work, GZO/CdS bilayer films prepared by magnetron sputtering were deposited on p-Si wafer to fabricate GZO/CdS/p-Si structure heterojunction device. The characterizations of the GZO/CdS bilayer films were carried out by X-ray diffraction (XRD), scanning electron microscope (SEM), X-ray photoelectron spectroscopy (XPS), ultraviolet-visible (UV-Vis) spectrophotometer and Hall effect measurement. The electrical GZO/CdS/p-Si heterojunction properties were investiga-

ted by current-voltage (*I-V*) measurement.

## 1 Experiment

For the purpose of fabricating GZO/CdS/p-Si structure heterojunction, p-type polished Si wafer was used as the substrate of the heterojunction. The thickness of the wafer used was 300  $\mu\text{m}$  and the crystal orientation was (100). The wafer was prepared by a standard cleaning procedure, then it was dipped in 10% HF solution for one minute to remove native oxide layer. Finally, the wafer was dried in a flow of nitrogen.

By thermal evaporation, 1  $\mu\text{m}$ -thick Al electrode was deposited on the back side.

CdS layer was deposited on p-Si substrate by radio-frequency (RF) magnetron sputtering. The CdS ceramic target was fabricated through hot pressed sintering. CdS power was used. The purity of the target is 99.99% and the size is  $\Phi$  60mm  $\times$  4mm. The distance between the target and the substrate was 5 cm. The base pressure inside the chamber was pumped down to less than  $5 \times 10^{-4}$  Pa. Sputtering was carried out at a working gas (pure Ar) pressure of 1 Pa. The Ar gas flow ratio was 80 sccm. The RF power and the temperature on substrates were kept at 80 W and 300°C, respectively. The sputtering was proceeded for 15min. The thickness of CdS film is about 200 nm.

GZO thin film was deposited on CdS/p-Si substrate by direct-current (DC) magnetron sputtering. The target was sintered ceramic disks of ZnO doped with 2 wt% Ga<sub>2</sub>O<sub>3</sub> (purity 99.99%). The base pressure inside the chamber was pumped down to less than  $5 \times 10^{-4}$  Pa. Sputtering was carried out at a working gas (pure Ar) pressure of 1 Pa. The Ar flow ratio was 80 sccm. The DC power and the temperature on substrates were kept at 60 W and 300°C, respectively. The sputtering was proceeded for 30 min. The thickness of GZO film is about 500 nm.

Finally, by coating, Ag paste was deposited on the top side of GZO/CdS/p-Si heterojunction. The area of the device is 0.5 cm<sup>2</sup>.

Microstructure of the GZO/CdS bilayer films was investigated by XRD, SEM and XPS. The optical transmission of the GZO/CdS films was measured by a UV-VIS spectrophotometer (Lambda35). The electrical properties of the films were characterized by Hall effect measurement (Accent HL5500pc) at room temperature. The current-voltage (*I-V*) characteristics of the GZO/CdS/p-Si heterojunction device were measured by Agilent 4155C semiconductor parameter analyzer at dark and under illumination of 100 mW/cm<sup>2</sup> (AM1.5) simulated light.

## 2 Results and discussion

### 2.1 Microstructural, optical and electrical properties of GZO/CdS bilayer films

Fig. 1 shows the XRD spectra of GZO/CdS bilayer films on glass in the range of  $2\theta = 20 \sim 60^\circ$ , which was

deposited by magnetron sputtering method. From these spectra, it was seen that the sample shows a polycrystalline phase. The XRD peak of  $34.18^\circ$  corresponds to Ga doped ZnO (002). In addition, the XRD peak of  $26.9^\circ$  corresponds to CdS (002). The result indicates that not only CdS film, but also GZO film has a hexagonal wurtzite structure with its dominant orientation strongly along the c-axis perpendicular to the substrate surface. The XRD peaks of CdS and GZO are sharp, this indicates the high crystallinity of CdS and GZO films.

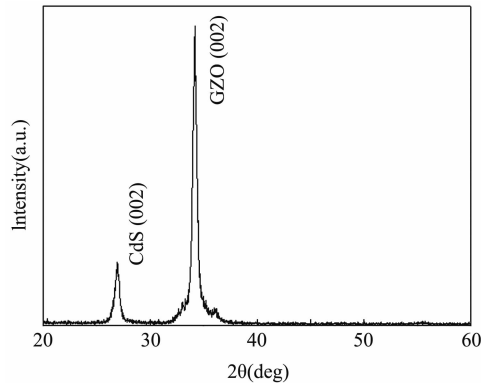


Fig. 1 XRD spectra of the GZO/CdS bilayer films  
图1 GZO/CdS 薄膜 XRD 谱

Fig. 2 shows the SEM images of the surface and cross-section of GZO/CdS bilayer thin films deposited by magnetron sputtering on p-Si substrate. Fig. 2 (a)-(d) show the film surface is dense and continuous. They indicate that the film consists of compact structure grains with sub-micron size and low roughness. The GZO film has the hilly shaped grains. It can be easily seen that the grains are tightly packed and the size varies from 100 to 300 nm. Fig. 2 (e)-(h) show the cross-sectional SEM images of the GZO/CdS structure. The CdS thin film deposited on the p-Si wafer exhibits densely packed crystals. The GZO/CdS films deposited on the p-Si substrate exhibits good coverage and densely packed crystal. They show that columnar GZO structure grew on the CdS/p-Si substrate. The average thickness of the CdS and GZO was about 200 nm and 500 nm, respectively.

XPS was used to study the elemental compositions. Fig. 3 (a) shows the X-ray photoelectron spectroscopy (XPS) survey scan of GZO/CdS bilayer films on Si substrate. It is obviously that there are Ga 3d, Zn 2p and O 1s peaks. The intensity of Ga 3d peak is obvious. A peak at 22.28 eV is detected in Ga 3d XPS spectrum (Fig. 3 (b)). The Zn  $2p_{3/2}$  and Zn  $2p_{1/2}$  peaks shown in Fig. 3(c) are located at 1020.88 eV and 1043.88 eV, respectively, with a peak splitting of 23 eV, which indicates the presence of  $Zn^{2+}$  state [15]. In Fig. 3(d), the O 1s peak located at 529.78 eV shows chemisorbed oxygen. The XPS study indicated the sample contains Ga, Zn and O. It is in agreement with XRD study.

Fig. 4 shows the optical transmittance spectra in the wavelength range of 300 ~ 900 nm of the GZO/CdS bilayer films deposited on glass substrate. The average transmittance of the GZO/CdS bilayer films is about 80% in the visible region. The GZO/CdS bilayer films exhibit a

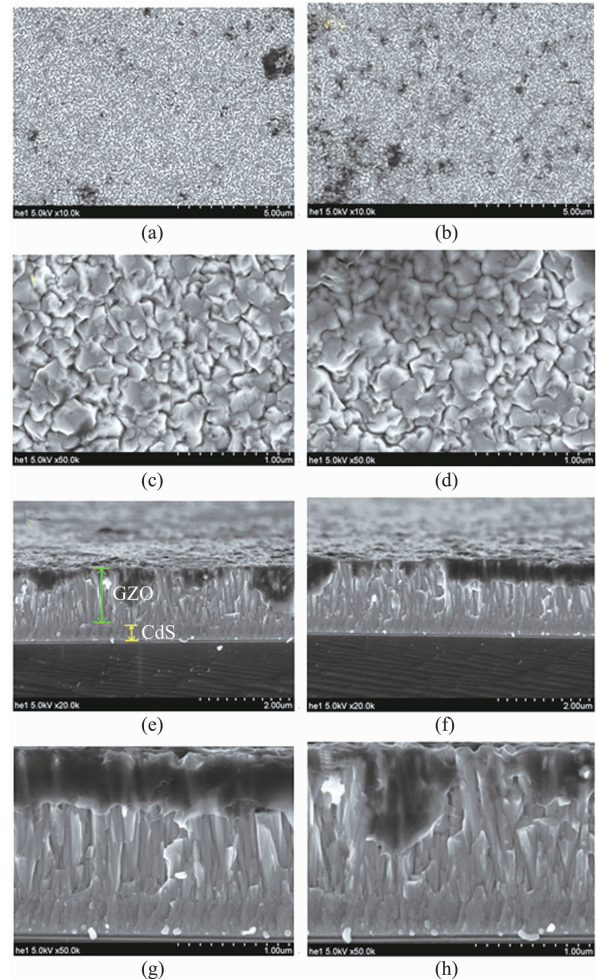


Fig. 2 The SEM images of the GZO/CdS bilayer films (a)-(d) surface (e)-(h) cross-section view

图2 GZO/CdS 薄膜的 SEM 照片 (a)-(d) 表面形貌 (e)-(h) 剖面图

sharp absorption edge in the 400 ~ 450 nm region. This is due to the absorption of GZO/CdS bilayer films. The energy bandgap of CdS is 2.4 eV. The wavelength of CdS absorption edge is 516 nm.

Electrical properties of the GZO/CdS bilayer films were measured by Hall effect measurement. It is a n-type semiconductor. The resistivity is  $5.836 \times 10^{-2} \Omega \cdot \text{cm}$ , the electron concentration and mobility are  $2.208 \times 10^{19} \text{ atom/cm}^3$  and  $4.843 \text{ cm}^2/\text{V} \cdot \text{s}$ , respectively.

## 2.2 Device characteristics

Fig. 5 is the linear current-voltage ( $I$ - $V$ ) behaviors between the two Ag electrodes on the surface of the GZO/CdS films. The inset shows the schematic of the test structure. It indicates a good ohmic contact. The distance of the two Ag electrodes on the film is 1cm. Fig. 6 shows a typical  $J$ - $V$  characteristic of the GZO/CdS/p-Si heterojunction device measured at room temperature in dark. The inset in Fig. 6 shows the heterojunction device structure and image. The  $J$ - $V$  curve of device shows an evident diode-like behavior. A small leakage current is observed in the reverse bias region, but the forward current is much higher than the reverse current. And the rectification ratios of  $I_F/I_R$  ( $I_F$  and  $I_R$

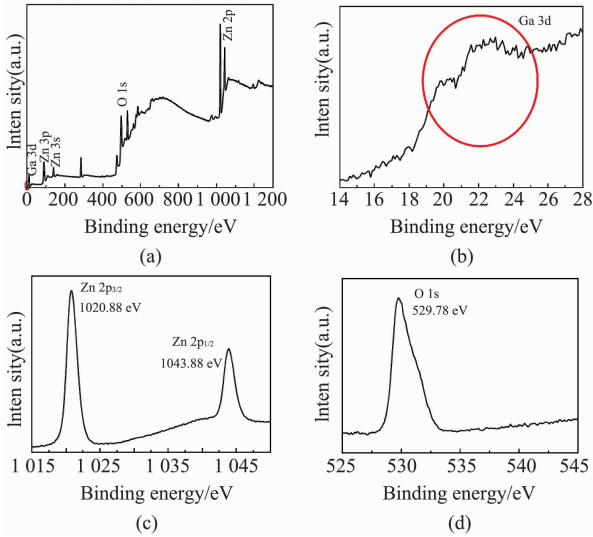


Fig. 3 XPS spectra of the GZO/CdS bilayer films on surface (a) surveyscan, (b) core-level spectrum for Ga 3d, (c) core-level spectrum for Zn 2p, (d) core-level spectrum for O 1s  
图3 GZO/CdS 薄膜的 XPS 谱(a)全谱图, (b) Ga 3d 精细谱, (c) Zn 2p 精细谱, (d) O 1s 精细谱

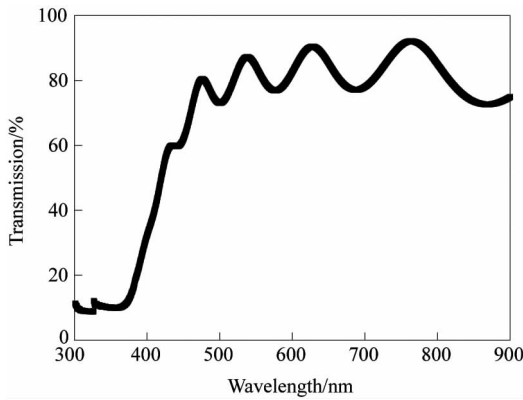


Fig. 4 Optical transmittance of the GZO/CdS bilayer films  
图4 GZO/CdS 薄膜的光学透射谱

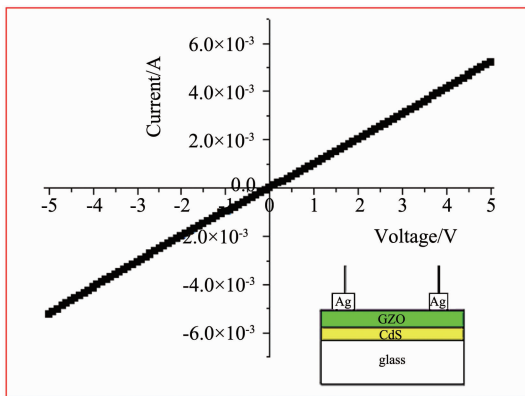


Fig. 5 *I-V* characteristic of Ag ohmic contacts to the GZO/CdS films  
图5 GZO/CdS 薄膜的银电极欧姆接触 *I-V* 曲线

stand for forward and reverse current, respectively) at  $\pm 3$  V is found to be as high as 21. The results indicate

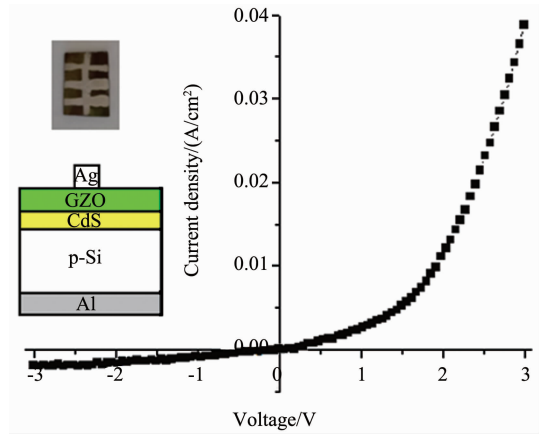


Fig. 6 *J-V* characteristic of the GZO/CdS/p-Si heterojunction in dark  
图6 无光照 GZO/CdS/p-Si 异质结 *J-V* 曲线

that the GZO/CdS/p-Si heterojunction possesses good diode characteristic.

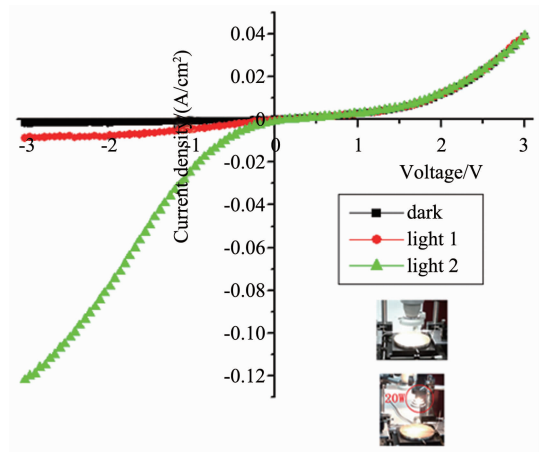


Fig. 7 *J-V* characteristic of the GZO/CdS/p-Si heterojunction in dark and in light (light 1:  $6.3 \text{ mW/cm}^2$  white light; Light 2: 20 W halogen lamp)  
图7 GZO/CdS/p-Si 异质结无光照及光照( $6.3 \text{ mW/cm}^2$  白光 LED 及 20 W 卤钨灯)条件下 *J-V* 曲线

The photo *J-V* characteristics were measured under illumination by low power white light ( $6.3 \text{ mW/cm}^2$ ) lamp and 20 W halogen lamp. The representative dark and photo *J-V* characteristics for the GZO/CdS/p-Si heterojunction are shown in Fig. 7. Typical rectifying and photoelectric behavior were observed for the device. The dark leakage current density is small, whereas its photocurrent density generated under illumination is much higher. For example, when the reverse bias is  $-3 \text{ V}$ , the dark current density is only  $1.88 \times 10^{-3} \text{ A/cm}^2$ . While the photocurrent reach to  $8.78 \times 10^{-3} \text{ A/cm}^2$  and  $1.22 \times 10^{-1} \text{ A/cm}^2$  in low power white light lamp and halogen lamp, respectively. This is generally understood that the photoelectric effect results from the light-induced electron generation at the depletion area of the p-Si, particularly near the heterojunction interface.

CdS absorbs UV photons, and p-Si absorbs lower

energy photons to generate electron-hole pairs. The built-in potential at the interface of CdS and Si derives the generated electrons and holes, so electrons and holes are separated at the junction. The photocurrents are consequently obtained.

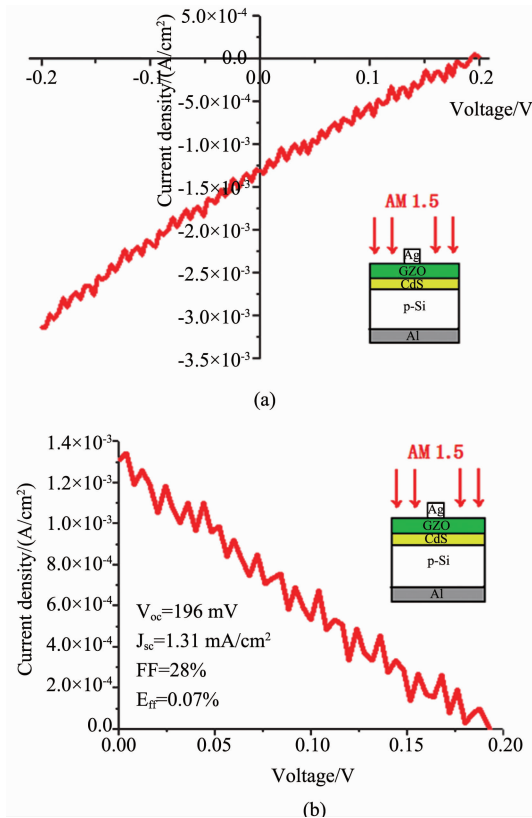


Fig. 8 (a)  $J$ - $V$  characteristic of the GZO/CdS/p-Si heterojunction under AM1.5 spectrum ( $100 \text{ mW/cm}^2$ ) condition (b) photoelectric efficiency of the GZO/CdS/p-Si heterojunction

图 8 (a) AM1.5 ( $100 \text{ mW/cm}^2$ ) 光照条件下, GZO/CdS/p-Si 异质结  $J$ - $V$  曲线 (b) GZO/CdS/p-Si 异质结的光电转换效率

The GZO/CdS/p-Si heterojunction performance was measured under AM1.5 illumination with a solar intensity of  $100 \text{ mW/cm}^2$  at  $25^\circ\text{C}$ . The current density ( $J$ )-voltage ( $V$ ) curve of the GZO/CdS/p-Si heterojunction measured under  $100 \text{ mW/cm}^2$  illumination (AM1.5 condition) is shown in Fig. 8(a). The device exhibits clear photovoltaic effect and the open-circuit voltage ( $V_{oc}$ ), short-circuit current density ( $J_{sc}$ ), fill factor (FF) and calculated power conversion efficiency ( $E_{ff}$ ) of the device are  $196 \text{ mV}$ ,  $1.31 \text{ mA/cm}^2$ ,  $28\%$  and  $0.07\%$ , respectively (Fig. 8 (b)). The result indicated that the GZO/CdS/p-Si heterojunction is an attractive candidate for low-cost photovoltaic applications in the future.

However, we could not observe any photovoltaic effect of GZO/p-Si heterojunction solar cell, which did not contain a CdS buffer layer (Fig. 9). Fig. 10 and Table. 1 show the crystal structure of GZO, CdS and Si. The ZnO:Ga is wurtzite structure, while the crystal structure of silicon is diamond structure. The lattice constant of

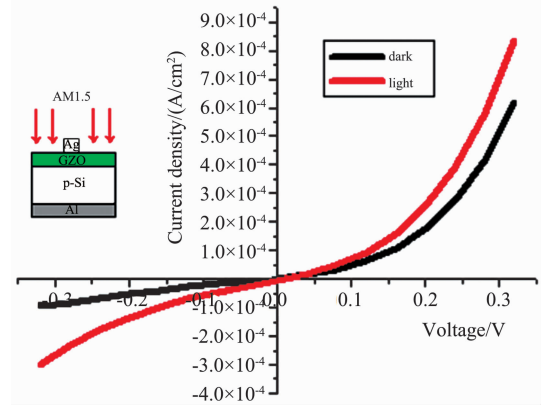


Fig. 9  $J$ - $V$  characteristic of the GZO/p-Si heterojunction under AM1.5 spectrum ( $100 \text{ mW/cm}^2$ ) condition  
图 9 AM1.5 ( $100 \text{ mW/cm}^2$ ) 光照条件下, GZO/p-Si 异质结  $J$ - $V$  曲线

GZO is  $3.25 \text{ \AA}$ , while the lattice constant of Si is  $5.42 \text{ \AA}$ . The lattice mismatch between GZO and Si is as high as  $40\%$ . There are so many interface states between GZO and p-Si. CdS is an n type semiconductor, and the crystal structure is wurtzite structure. The lattice constant of CdS is  $4.14 \text{ \AA}$ , which is between GZO and Si. Therefore, it can be used for a buffer layer between GZO and Si, and it can also effectively reduce the interface states between GZO and p-Si. So we observed the clear photovoltaic effect of GZO/CdS/p-Si heterojunction.

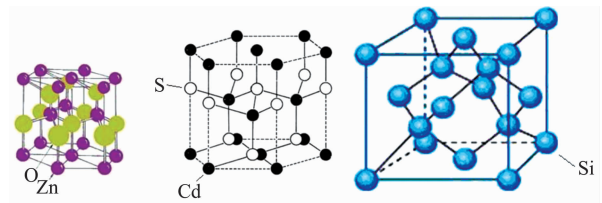


Fig. 10 The crystal structure of GZO, CdS and Si  
图 10 GZO, CdS, Si 的晶体结构

Table 1  
表 1

material	crystal structure	lattice constant	Bandgap
ZnO:Ga	wurtzite structure	a $3.25 \text{ \AA}$ c $5.21 \text{ \AA}$	$3.3 \text{ eV}$
CdS	wurtzite structure	a $4.14 \text{ \AA}$ c $6.72 \text{ \AA}$	$2.4 \text{ eV}$
Si	diamond structure	$5.43 \text{ \AA}$	$1.12 \text{ eV}$

The incident light can pass through the GZO/CdS double films, then be absorbed by the p-Si wafer to generate photoinduced electrons and holes pairs. Because the workfunction of GZO is lower than the p-Si substrate, a built-in field is near the surface of p-Si wafer. As shown in Fig. 11, the photogenerated electrons can be swept to the GZO side and the photogenerated holes can be swept to the p-Si side<sup>[16]</sup>. We can find the clear photovoltaic and photoelectric effect.

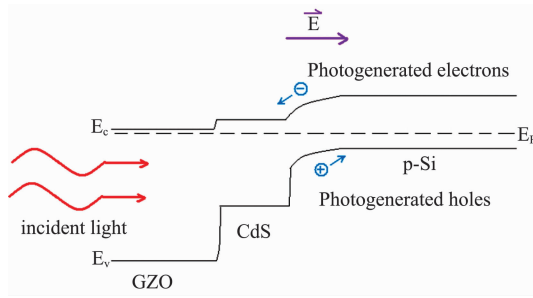


Fig. 11 The bandgap of GZO/CdS/p-Si heterojunction solar cell under light illumination

图 11 GZO/CdS/p-Si 异质结光照下的能带图

### 3 Conclusion

The GZO/CdS/p-Si heterojunction photoelectric device has been fabricated successfully by depositing highly c-axis oriented GZO/CdS films on p-Si (100) wafer using magnetron sputtering. The structural, optical and electrical properties of GZO/CdS films were studied by XRD, SEM, XPS, UV-VIS spectrophotometer and Hall effect measurement. From optical transmittance measurement, the average transmittance of the GZO/CdS bilayer films is about 80% in the visible region. The J-V curve of GZO/CdS/p-Si heterojunction device shows good rectifying behavior. And the value of  $I_F/I_R$  ( $I_F$  and  $I_R$  stand for forward and reverse current, respectively) at  $\pm 3$  V is found to be as high as 21. The results indicate that the nanocrystalline GZO/CdS/p-Si heterojunction possesses good diode characteristic. High photocurrent is obtained under a reverse bias. The lattice constant of CdS is between GZO and Si, so it can be used for a buffer layer between GZO and Si, to effectively reduce the interface states between GZO and p-Si. The GZO/CdS/p-Si heterojunction device exhibits clear photovoltaic effect. Under an AM1.5 illumination condition, the open-circuit voltage ( $V_{oc}$ ), short-circuit current density ( $J_{sc}$ ), fill factor (FF) and calculated power conversion efficiency ( $\eta$ ) are 196 mV, 1.31 mA/cm<sup>2</sup>, 28% and 0.07%, respectively. The above results indicate that the GZO/CdS/p-Si heterojunction suggests wider applications for low-cost solar cell and photodetector in the future.

### Acknowledgment

The project was supported by the fund of PLA General Armament Department “The 13th Five-year” Weapons and Equipments Pre-research Field Foundation “Basic application technology of graphene materials in batteries” (6140721040412), The Fundamental Research Funds for the Central Universities, China, Dong Hua University (2232016D3-08 and 2232016D3-03), The fund of Shanghai alliance project (Shanghai Municipal Science and technology achievements transformation Promotion Association, Shanghai Educational Development Foundation and Shanghai city to promote the transformation of scientific and technological achievements Foundation. Grant No. LM201601). The fund of Norwegian Research

Council (NRC) project “Crucibles for next generation high quality silicon solar cells” (CruGenSi, No. 268027). The first author of this paper was funded by the Norwegian Research Council (NRC) project in the Solar Energy Department at Institute for Energy Technology (Norway) for half a year as a visiting researcher from January 2018 to July 2018.

### References

- [1] Du H W, Yang J, Li Y H, *et al.* Preparation of ITO/SiOx/n-Si solar cells with non-decline potential field and hole tunneling by magnetron sputtering [J]. *Applied Physics Letters*, 2015, **106**: 093508.
- [2] Shen L, Ma Z Q, Shen C, *et al.* Studies on fabrication and characterization of a ZnO/p-Si-based solar cell [J]. *Superlattices and Microstructures*, 2010, **48**: 426–433.
- [3] Poonam Shokeen, Amit Jain, Avinashi Kapoor, Plasmonic ZnO/p-silicon heterojunction solar cell [J]. *Optical Materials*, 2017, **67**: 32–37.
- [4] Bo He, Jing Xu, Huai Zhong Xing, *et al.* The effect of substrate temperature on high quality c-axis oriented AZO thin films prepared by DC reactive magnetron sputtering for photoelectric device applications [J]. *Superlattices and Microstructures*, 2013, **64**: 319–330.
- [5] Wang Lia, YingyiLi, GuopingDu. Enhanced electrical and optical properties of boron-doped ZnO films grown by low pressure chemical vapor deposition for amorphous silicon solar cells [J]. *Ceramics International*, 2016, **42**: 1361–1365.
- [6] Wen B, Liu C Q, Wang N. Properties of transparent conductive boron-doped ZnO thin films deposited by pulsed DC magnetron sputtering from Zn<sub>1-x</sub>B<sub>x</sub>O targets [J]. *Applied Physics A*, 2017, **123**: 211.
- [7] Anil Singh, Sujeet Chaudhary, D. K. Pandya, High conductivity indium doped ZnO films by metal target reactive co-sputtering [J]. *Acta Materialia*, 2016 **111**: 1–9.
- [8] Hyun-Woo Parka, Kwun-BumChungb, Jin-SeongParkb. Electronic structure of conducting Al-doped ZnO films as a function of Al doping concentration [J]. *Ceramics International*, 2015, **41**: 1641–1645.
- [9] ShuqunChen, MichaelE. A. Warwick, Effects of film thickness and thermal treatment on the structural and opto-electronic properties of Ga-doped ZnO films deposited by sol-gel method [J]. *Solar Energy Materials & Solar Cells*, 2015, **137**: 202–209.
- [10] Donguk Kim, Young Park, Minha Kim, Optical and structural properties of sputtered CdS films for thin film solar cell applications [J]. *Materials Research Bulletin*, 2015, **69**: 78–83.
- [11] Bo Liu, Run Luo, Bing Li. Effects of deposition temperature and CdCl<sub>2</sub> annealing on the CdS thin films prepared by pulsed laser deposition [J]. *Journal of Alloys and Compounds*, 2016, **654**: 333–339.
- [12] Sivaraman T, Narasimman V, Nagarethinam V S. Effect of chlorine doping on the structural, morphological, optical and electrical properties of spray deposited CdS thin films [J]. *Progress in Natural Science: Materials International*, 2015, **25**: 392–398.
- [13] Abdolhazadeh Ziabari A, Ghodsi F E. Influence of Cu doping and post-heat treatment on the microstructure, optical properties and photoluminescence features of sol-gel derived nanostructured CdS thin films [J]. *Journal of Luminescence*, 2013, **141**: 121–129.
- [14] LI L, SHAN C X, LI B H. Light-Harvesting in n-ZnO/p-Silicon Heterojunctions [J]. *Journal of ELECTRONIC MATERIALS*, 2010, **39**: 2467–2470.
- [15] Daza L G, Martin-Tovar I E A, Castro-Rodriguez R. Aluminum-Doped Zinc Oxide Thin Films Deposited on Flexible Cellulose Triacetate Substrates Prepared by RF Sputtering [J]. *J Inorg Organomet Polym*, 2017, **27**: 1563–1571.
- [16] Bo He, Jing Xu, HuanPo Ning *et al.* Optoelectronic properties of SnO<sub>2</sub>/p-Si heterojunction prepared by a simple chemical bath deposition method [J]. *J. infrared millim. Waves*, 2017, **36**(2): 139–143.